

Modern Physics Letters A
 © World Scientific Publishing Company

Semileptonic B Decays and Determination of $|V_{ub}|$

MASAHIRO MORII

*Department of Physics, Harvard University, 17 Oxford Street
 Cambridge, Massachusetts 02138, USA
 morii@fas.harvard.edu*

Received (Day Month Year)

Revised (Day Month Year)

Semileptonic decays of the B mesons provide an excellent probe for the weak and strong interactions of the bottom quark. The large data samples collected at the B Factories have pushed the experimental studies of the semileptonic B decays to a new height and stimulated significant theoretical developments. I review recent progresses in this fast-evolving field, with an emphasis on the determination of the magnitude of the Cabibbo-Kobayashi-Maskawa matrix element $|V_{ub}|$.

Keywords: Semileptonic B decays; CKM matrix; $|V_{ub}|$

PACS Nos.: 12.15.Hh, 13.20.He, 14.40.Nd

1. Introduction

The success of the B Factories, PEP-II and KEKB, has dramatically improved our understanding of the CP violation. The latest results of the time-dependent CP asymmetries in the neutral B decays are in good agreement with the predictions of the Cabibbo-Kobayashi-Maskawa mechanism¹ as shown in Fig. 1. The precision of the consistency test is no longer limited by the measurement of the CP -violating parameter $\sin 2\beta$, but by the measured ratio of the Cabibbo-Kobayashi-Maskawa (CKM) matrix elements $|V_{ub}/V_{cb}|$, which determines the length of the left side of the Unitarity Triangle. The current uncertainties of $|V_{ub}|$ and $|V_{cb}|$ are $\geq 10\%$ and $\sim 2\%$, respectively. Improvement of our knowledge of $|V_{ub}|$ will directly translate to a more stringent test of the Standard Model.

Semileptonic decays of B mesons provide a clean environment for studying the tree decay amplitudes, which allows us to determine $|V_{ub}|$ and $|V_{cb}|$. Experimental studies of charmless semileptonic B decays can be broadly categorized into *inclusive* and *exclusive* measurements. The former measures the decay rate $\Gamma(B \rightarrow X_u \ell \nu)$, where X_u is a hadronic system without charm content.^a The latter measures the

^aThroughout this article, the symbol $\ell \nu$ stands for $e^- \bar{\nu}_e$, $\mu^- \bar{\nu}_\mu$, or their charge-conjugation partners.

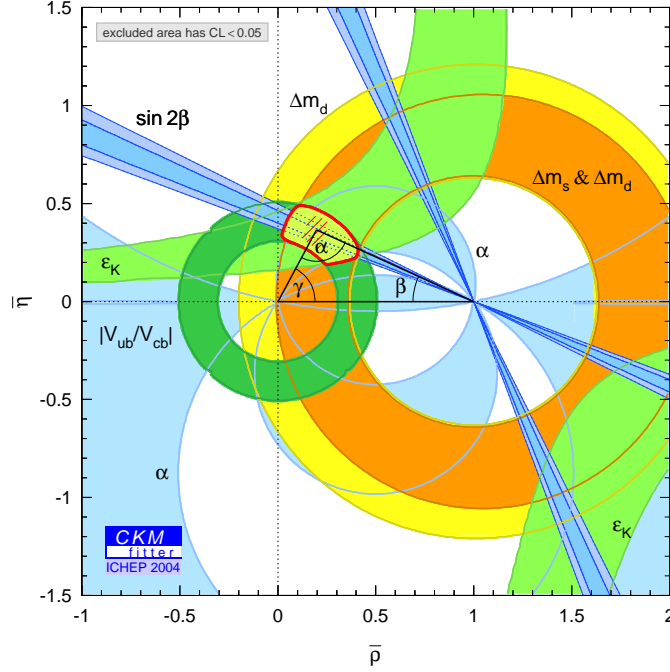


Fig. 1. Global fit of the experimental data as of summer 2004 by the CKMfitter.² The red contour contains the 95% C.L. region based on the measurements of ε_K , $|V_{ub}/V_{cb}|$, Δm_d , and the lower limit on Δm_s . The green ring centered around (0,0) is the 95% C.L. region based on $|V_{ub}/V_{cb}|$.

decay rates for exclusive final states such as $B \rightarrow \pi \ell \nu$ and $\rho \ell \nu$. In addition to having different efficiencies and signal-to-background ratios, the inclusive and exclusive measurements depend on different types of theoretical calculations. Pursuing both approaches and comparing the results will help us verify the robustness of the theoretical errors, which limit the current precision of $|V_{ub}|$.

The experimental and theoretical issues surrounding the determination of $|V_{ub}|$ are complex and sometimes controversial. Progress in the last few years nonetheless has made it a concrete possibility that $|V_{ub}|$ will soon be determined with a precision of 10% or better. In this article, I review the current status of the measurements and discuss potential improvements that can be achieved in the near future.

2. Inclusive Measurement of $|V_{ub}|$

In an inclusive measurement of $|V_{ub}|$, one measures the rate of the charmless semileptonic decay $B \rightarrow X_u \ell \nu$ without reconstructing the hadronic system X_u . Since the u quark is much lighter than the c quark, the $B \rightarrow X_u \ell \nu$ signal can be statistically separated from the more copious $B \rightarrow X_c \ell \nu$ background taking advantage of the differences in the decay kinematics.

2.1. Theoretical Background

Quark-hadron duality³ connects the inclusive decay width $\Gamma(B \rightarrow X_u \ell \nu)$ to the quark-level decay width

$$\Gamma(b \rightarrow u \ell \nu) = \frac{G_F^2 |V_{ub}|^2}{192 \pi^3} m_b^5. \quad (1)$$

The effect of the spectator quark is calculated using the Operator Product Expansion (OPE), which expands the QCD corrections in powers of $\alpha_s(m_b)$ and of Λ_{QCD}/m_b . The former, perturbative, corrections have been calculated to $O(\alpha_s^2)$.⁴ The latter, non-perturbative, corrections start at $O(\Lambda_{\text{QCD}}^2/m_b^2)$. The leading term appears as $(\lambda_1 - 9\lambda_2)/(2m_b^2)$, where λ_1 and λ_2 are the parameters due to the b quark's Fermi motion and the hyperfine interaction between the b and light quarks, respectively. The non-perturbative parameters λ_1 and λ_2 are known from the measurements of $B \rightarrow X_c \ell \nu$ decays and, in the case of λ_2 , from the B - B^* mass difference. Overall, the uncertainties in $\Gamma(B \rightarrow X_u \ell \nu)$ due to the QCD corrections are small compared with the uncertainty due to the b quark mass, which appears as m_b^5 in (1).

The same OPE framework applied to the $B \rightarrow X_c \ell \nu$ decays can predict $\Gamma(B \rightarrow X_c \ell \nu)$ and the moments of the kinematical variables such as the lepton energy E_ℓ and the hadronic mass m_X in terms of $|V_{cb}|$, $\alpha_s(m_b)$, m_b , m_c and the non-perturbative parameters. By measuring the inclusive rate and several of the E_ℓ and m_X moments as functions of the minimum lepton energy, *BABAR*⁵ determined $|V_{cb}|$, m_b , m_c , and the non-perturbative parameters from a simultaneous fit to the OPE calculation. The results are

$$\begin{aligned} |V_{cb}| &= (41.4 \pm 0.4 \pm 0.4 \pm 0.6) \times 10^{-3}, \\ m_b &= (4.61 \pm 0.05 \pm 0.04 \pm 0.02) \text{ GeV}, \\ m_c &= (1.18 \pm 0.07 \pm 0.06 \pm 0.02) \text{ GeV}, \\ \mu_\pi^2 &= (0.45 \pm 0.04 \pm 0.04 \pm 0.01) \text{ GeV}^2, \\ \mu_G^2 &= (0.27 \pm 0.06 \pm 0.03 \pm 0.02) \text{ GeV}^2, \end{aligned}$$

where the errors are experimental, uncertainties in the OPE calculation, and other theoretical uncertainties, respectively. The parameters μ_π^2 and μ_G^2 are related to λ_1 and λ_2 , respectively. The quark masses and the non-perturbative parameters depend on the quark mass scheme and the renormalization scale used in the OPE calculation; the calculation⁶ adopted in this analysis employed the kinetic scheme,⁷ in which the non-perturbative contribution to the b -quark mass is subtracted using heavy-quark sum rules, with the scale $\mu = 1.0 \text{ GeV}$. The fit describes the data points quite well with $\chi^2 = 20$ for 15 degrees of freedom. Bauer *et al.*⁸ have performed a more extensive global fit using measurements from *BABAR*, *Belle*, *CLEO*, *CDF*, and *DELPHI*. Using the $1S$ scheme,⁹ which relates the b -quark mass to the mass of the $\Upsilon(1S)$ resonance, they find $|V_{cb}| = (41.4 \pm 0.6 \pm 0.1) \times 10^{-3}$, where the first error includes both experimental and theoretical uncertainties and the second error is due

to the B meson lifetime. Bauer *et al.* repeat the fit with different expansion and mass schemes and find good agreement. In addition to determining $|V_{cb}|$ to a 2% precision, these fits demonstrate the reliability of the OPE framework in predicting the inclusive decay rate and spectral moments.

Because of the presence of the $B \rightarrow X_c \ell \nu$ background, the inclusive $B \rightarrow X_u \ell \nu$ decay width cannot be directly measured. The experiments measure, instead, partial decay widths in limited regions of the phase space that are free from the $B \rightarrow X_c \ell \nu$ background. This is achieved by a cut on one or more of the three kinematic variables of the $X \ell \nu$ final state: the lepton energy E_ℓ , the hadronic mass m_X , and the lepton-neutrino invariant mass squared q^2 . The fraction, f_u , of the $B \rightarrow X_u \ell \nu$ events that pass the experimental cut needs to be accurately known in order to determine $|V_{ub}|$.

The OPE framework can reliably predict the inclusive $B \rightarrow X_u \ell \nu$ decay rate as long as it is integrated over a large region of the phase space. The experimental cuts required to suppress the $B \rightarrow X_c \ell \nu$ background violate this requirement. In order to overcome this limitation, a so-called twist expansion¹⁰ is performed. The leading term of the non-perturbative correction becomes $O(\Lambda_{\text{QCD}}/m_b)$ instead of $O(\Lambda_{\text{QCD}}^2/m_b^2)$, and is described by the distribution function, known as the *shape function*, of the light-cone momentum of the b quark inside the B meson.

The shape function cannot be computed perturbatively, and must be determined experimentally. This is achieved by two methods:

- The first and second moments of the shape function are related to $\bar{\Lambda} = m_B - m_b$ and λ_1 , which are determined by the OPE fit to the $B \rightarrow X_c \ell \nu$ moments. The recent two-loop calculation by Neubert¹¹ allows the translation of m_b and μ_π^2 determined in various mass schemes into the shape-function scheme. Using the results from the BABAR OPE fit discussed above, Neubert finds $m_b = (4.63 \pm 0.08) \text{ GeV}$ and $\mu_\pi^2 = (0.15 \pm 0.07) \text{ GeV}^2$ at the renormalization scale $\mu = 1.5 \text{ GeV}$.
- The photon energy spectrum in the $b \rightarrow s \gamma$ decays is affected, in the leading order of Λ_{QCD}/m_b , by the same shape function. The $b \rightarrow s \gamma$ measurements by CLEO,¹² Belle,¹³ and BABAR¹⁴ are used to constrain $\bar{\Lambda}$ and λ_1 . The latest BABAR measurement using the sum of exclusive $B \rightarrow X_s \gamma$ decays finds $m_b = (4.65 \pm 0.04) \text{ GeV}$ and $\mu_\pi^2 = (0.19 \pm 0.06) \text{ GeV}^2$ in the shape-function scheme with $\mu = 1.5 \text{ GeV}$.

The good agreement between the results obtained by the two independent methods suggests that the theoretical uncertainties are under control.

In most of the $B \rightarrow X_u \ell \nu$ events that are experimentally accessible, the hadronic system X_u has a small mass and large momentum, i.e., it is jet-like. The suitable theoretical tool, Soft Collinear Effective Theory (SCET) has been developed in the last few years.¹⁵ Recent theoretical analyses of the $B \rightarrow X_u \ell \nu$ and $b \rightarrow s \gamma$ decays use SCET. Until recently, the experiments relied on an $O(\alpha_s)$ OPE calculation by De Fazio and Neubert¹⁶ to evaluate the acceptance f_u of their event selection criteria. Latest results of $|V_{ub}|$ extracted from inclusive measurements use a new SCET-based calculation by Bosch *et al.*^{17,18} The new calculation tends to predict

slightly larger f_u than the previous calculation. More importantly, the values of f_u depend more strongly on the shape-function parameters, making them the largest source of uncertainty on $|V_{ub}|$ as it will be seen in Section 2.3.

Beyond the shape-function uncertainty, which we can expect to improve with better measurements of $B \rightarrow X_c \ell \nu$ and $b \rightarrow s \gamma$, a few theoretical issues remain unresolved:

- The $B \rightarrow X_u \ell \nu$ and $b \rightarrow s \gamma$ processes are governed by the single shape function only in the leading order of Λ_{QCD}/m_b , and the next-to-leading order corrections differ. The impact of the sub-leading shape functions is a subject of active theoretical research.¹⁹
- For $B^0 \rightarrow X_u \ell \nu$, additional complication arises from the weak-annihilation diagram,²⁰ in which the b and \bar{d} quarks annihilate into a W^- boson. The contribution to the total rate is expected to be small ($\leq 2\%$), but concentrated near the lepton-energy endpoint where its relative contribution may be significant. The size of the effect of the weak annihilation can be constrained in the future by measuring the lepton spectrum separately for $B^0 \rightarrow X_u \ell \nu$ and $B^+ \rightarrow X_u \ell \nu$. Alternatively, a cut that rejects the highest- q^2 region, as proposed by Lange *et al.*,¹⁸ can be used to suppress the effect of the weak annihilation.

The current estimates of these uncertainties contribute to a theoretical error of $\sim 5\%$ on $|V_{ub}|$. Understanding of these issues will become important as we improve the experimental and shape-function errors in the next few years.

2.2. Experimental Measurements

Recent inclusive measurements of $|V_{ub}|$ use one of the three techniques:

- The lepton endpoint measurements^{21,22} use the momentum spectrum of the leptons near the kinematical endpoint.
- The neutrino reconstruction measurement²³ estimates the neutrino momentum from the missing momentum of the event.
- The hadronic recoil measurements^{24,25} use the recoil of the B mesons that are fully reconstructed in hadronic decays.

The upper endpoint region of the lepton-energy spectrum offers the most accessible window to the $B \rightarrow X_u \ell \nu$ signal. The earliest measurements of the $B \rightarrow X_u \ell \nu$ decay by CLEO²⁶ and ARGUS²⁷ used leptons with momenta beyond the kinematical endpoint for the $B \rightarrow X_c \ell \nu$ decay. The available phase space above the charm endpoint is unfortunately small ($f_u \approx 6\%$) and extends beyond the quark-level endpoint. The accessible signal fraction f_u is therefore strongly dependent on the shape function. The signal rate near the endpoint is also sensitive to the weak-annihilation effect. These factors make it difficult to evaluate reliably the theoretical uncertainty of f_u for an endpoint measurement.

Recent measurements of $|V_{ub}|$ using the E_ℓ spectrum try to ameliorate the theoretical issues by extending the signal region significantly below the $B \rightarrow X_c \ell \nu$ endpoint. *BABAR*²¹ and Belle²² measured the partial branching fraction $\Delta\mathcal{B}(B \rightarrow X_u e \nu)$ for the electron momentum interval of 2.0–2.6 GeV and 1.9–2.6 GeV, respectively. The minimum lepton momentum in the previous measurements from CLEO²⁸ and Belle²⁹ were 2.2 GeV and 2.3 GeV, respectively. The accessible signal fraction f_u for $E_\ell > 2.0$ GeV is as large as 28%.

In order to achieve measurements far below the $B \rightarrow X_c \ell \nu$ threshold, accurate modeling and subtraction of the background, both $B \rightarrow X_c \ell \nu$ and non- $B\bar{B}$, are essential. The non- $B\bar{B}$ background is subtracted using off-peak data collected at center-of-mass energies below the $\Upsilon(4S)$ resonance. The E_e spectrum is then fitted with a combination of the $B \rightarrow X_u \ell \nu$ signal, $B \rightarrow D \ell \nu$, $B \rightarrow D^* \ell \nu$, $B \rightarrow D^{**} \ell \nu$, and non-resonant $B \rightarrow D^{(*)} \pi \ell \nu$ background distributions. The convergence of the fit is helped by the fact that the high end of the E_e spectrum is dominated by the D and D^* states. Extending the E_e ranges lower would require better understanding of the production of the higher D resonances and non-resonant semileptonic decays.

Using data samples corresponding to 80 fb^{-1} and 27 fb^{-1} , *BABAR* and Belle measure partial branching fractions

$$\begin{aligned}\Delta\mathcal{B}(p_e > 2.0 \text{ GeV}) &= (5.31 \pm 0.32 \pm 0.49) \times 10^{-4}, \\ \Delta\mathcal{B}(p_e > 1.9 \text{ GeV}) &= (8.47 \pm 0.37 \pm 1.53) \times 10^{-4},\end{aligned}$$

respectively, where the errors are statistical and systematic. The larger systematic error of the Belle result reflects the difficulty associated with understanding the increasing background at lower lepton energies.

The neutrino-reconstruction measurement by *BABAR*²³ combines electrons with $E_e > 1.9$ GeV with the neutrino momentum, inferred from the missing momentum of the event, to calculate the q^2 of the lepton-neutrino system. For a given set of (E_e, q^2) , the maximum hadronic mass squared can be calculated as

$$s_h^{\max} = m_B^2 + q^2 - 2m_B \left(E_e + \frac{q^2}{4E_e} \right), \quad (2)$$

plus a small correction to account for the B momentum in the $\Upsilon(4S)$ rest frame.³⁰ Requiring $s_h^{\max} < 3.5 \text{ GeV}^2$ removes a large fraction of the $B \rightarrow X_c \ell \nu$ background. *BABAR* achieves a signal-to-background ratio of 1/2 with a signal acceptance $f_u \sim 16\%$. The resolution of the s_h^{\max} variable is studied using a control sample of exclusively reconstructed $B \rightarrow D^{(*)} \ell \nu$ decays. The measured partial branching fraction is

$$\Delta\mathcal{B}(E_e > 1.9 \text{ GeV}, s_h^{\max} < 3.5 \text{ GeV}^2) = (4.46 \pm 0.42 \pm 0.83) \times 10^{-4},$$

where the errors are statistical and systematic. The data sample used corresponds to 80 fb^{-1} . The systematic error is expected to improve by the time the measurement is published.

The large signal acceptances of the m_X and q^2 cuts alleviate some of the theoretical difficulties encountered by the E_ℓ endpoint measurements. In principle, an m_X cut at the D meson mass provides the best signal acceptance possible ($f_u \approx 70\%$). The m_X spectrum, however, has a strong shape-function dependence near the D threshold, and so does f_u . A q^2 cut at $(m_B - m_D)^2$, on the other hand, provides a moderate efficiency ($f_u \approx 20\%$) with small dependence on the shape function. Two other cuts have been proposed to minimize the theoretical errors while maintaining good signal acceptance:

- Bauer *et al.*³¹ proposed a combined cut on both m_X and q^2 that would maximize f_u while minimizing its shape-function dependence. For a typical set of cuts at $m_X < 1.7 \text{ GeV}$ and $q^2 > 8 \text{ GeV}^2$, the acceptance f_u is around 30% with an uncertainty of $\sim 6\%$.
- Mannel and Recksiegel,³² and more recently Bosch *et al.*,^{17,33} proposed a cut on $P_+ = E_X - p_X$, where E_X and p_X are the energy and momentum of the hadronic system, respectively. A cut at $P_+ < m_D^2/m_B$ would have a large f_u of $\sim 60\%$ and reject the region where the SCET is not applicable.

In order to measure the hadronic mass m_X , one must identify all the decay products of the B meson. This is achieved in the hadronic-recoil measurements by *BABAR*²⁵ and *Belle*²⁴ by completely reconstructing one B meson and using the recoiling B meson. With full reconstruction of hadronic B decays, the four-momentum of the recoil B is known by momentum conservation. After finding a lepton candidate with $p_\ell > 1 \text{ GeV}$ in the recoil, a kinematical fit calculates the most likely four-momenta for the neutrino and for the hadronic system. The typical m_X resolution is 350 MeV. The $B \rightarrow X_c \ell \nu$ background is suppressed by the likely presence of kaons in the final state, and by finding soft pions that are kinematically consistent with the $B \rightarrow D^* \ell \nu$ decay.

The hadronic-recoil measurements can measure the partial branching ratio in a variety of regions of the (m_X, q^2) space. For $m_X < 1.7 \text{ GeV}$ and $q^2 > 8 \text{ GeV}^2$, *BABAR* and *Belle* find

$$\begin{aligned}\Delta\mathcal{B}(m_X < 1.7 \text{ GeV}, q^2 > 8 \text{ GeV}^2) &= (8.96 \pm 1.43 \pm 1.44) \times 10^{-4}, \\ \Delta\mathcal{B}(m_X < 1.7 \text{ GeV}, q^2 > 8 \text{ GeV}^2) &= (8.41 \pm 0.85 \pm 1.03) \times 10^{-4},\end{aligned}$$

respectively, where the errors are statistical and systematic. The data samples used are 80 fb^{-1} for *BABAR*, and 253 fb^{-1} for *Belle*. *Belle* has also measured the partial branching fraction

$$\Delta\mathcal{B}(P_+ < 0.66 \text{ GeV}) = (11.0 \pm 1.0 \pm 1.6) \times 10^{-4},$$

where the errors are statistical and systematic.

Table 1. Measured partial branching fractions $\Delta\mathcal{B}$ and the extracted values of $|V_{ub}|$. The errors on $\Delta\mathcal{B}$ are statistical and systematic. The errors on $|V_{ub}|$ are experimental, due to the shape function, and theoretical. The average excludes the Belle P_+ result.

Cuts		$\Delta\mathcal{B} \times 10^4$	$ V_{ub} \times 10^3$
BABAR	$E_\ell > 2.0 \text{ GeV}$	$5.3 \pm 0.3 \pm 0.5$	$3.93 \pm 0.34 \pm 0.38 \pm 0.18$
Belle	$E_\ell > 1.9 \text{ GeV}$	$8.5 \pm 0.4 \pm 1.5$	$4.50 \pm 0.42 \pm 0.32 \pm 0.21$
BABAR	$E_\ell > 1.9 \text{ GeV}, s_h^{\text{max}} < 3.5 \text{ GeV}^2$	$4.5 \pm 0.4 \pm 0.8$	$3.89 \pm 0.40 \pm 0.45 \pm 0.21$
BABAR	$m_X < 1.7 \text{ GeV}, q^2 > 8 \text{ GeV}^2$	$9.0 \pm 1.4 \pm 1.4$	$4.45 \pm 0.49 \pm 0.40 \pm 0.22$
Belle	$m_X < 1.7 \text{ GeV}, q^2 > 8 \text{ GeV}^2$	$8.4 \pm 0.9 \pm 1.0$	$4.34 \pm 0.34 \pm 0.33 \pm 0.22$
Belle	$P_+ < 0.66 \text{ GeV}$	$11.0 \pm 1.0 \pm 1.6$	$3.87 \pm 0.33 \pm 0.35 \pm 0.13$
Average $ V_{ub} $			$4.27 \pm 0.20 \pm 0.35 \pm 0.21$

2.3. Extraction of $|V_{ub}|$

The partial branching fractions measured by the experiments can be translated into $|V_{ub}|$ by

$$|V_{ub}| = \sqrt{\frac{\Delta\mathcal{B}}{\tilde{\Gamma}_{\text{thy}}\tau_B}}, \quad (3)$$

where τ_B is the average lifetime of B^0 and B^+ . The reduced decay rate $\tilde{\Gamma}_{\text{thy}}$ is defined as

$$\tilde{\Gamma}_{\text{thy}} \equiv \frac{\Delta\Gamma_{\text{thy}}}{|V_{ub}|^2}, \quad (4)$$

where $\Delta\Gamma_{\text{thy}}$ is the partial width of the $B \rightarrow X_u \ell \nu$ decay into the phase space of interest predicted by the theory.

Until recently, the conversion was often performed in two steps. The measured $\Delta\mathcal{B}$ was converted into the total branching fraction $\mathcal{B} = \Delta\mathcal{B}/f_u$, which was then converted into $|V_{ub}|$ using the OPE calculation for the fully inclusive decay rate $\Gamma(B \rightarrow X_u \ell \nu)$. Since both f_u and $\Gamma(B \rightarrow X_u \ell \nu)$ depend critically on m_b , care must be taken to treat the correlation in their uncertainties. Equation (3) avoids this problem by calculating the partial decay rate directly.¹⁸

Table 1 and Fig. 2 summarizes the values of $|V_{ub}|$ extracted by BABAR³⁴ and Belle²⁴ from the inclusive measurements. Both experiments used the calculation by Bosch *et al.*^{17,18} to evaluate $\tilde{\Gamma}_{\text{thy}}$. For the shape function parameters, BABAR used $m_b = (4.63 \pm 0.08) \text{ GeV}$ and $\mu_\pi^2 = (0.15 \pm 0.07) \text{ GeV}^2$ derived from the $B \rightarrow X_c \ell \nu$ OPE fit,¹¹ and Belle used $m_b = (4.63 \pm 0.07) \text{ GeV}$ and $\mu_\pi^2 = (0.20 \pm 0.07) \text{ GeV}^2$. The theoretical errors include perturbative errors, effects of the subleading shape functions and weak annihilation.

The existing measurements agree well with each other. Assuming that the experimental errors are uncorrelated and the shape function and theory errors are fully correlated, we find the average value

$$|V_{ub}| = (4.27 \pm 0.20 \pm 0.35 \pm 0.21) \times 10^{-3},$$

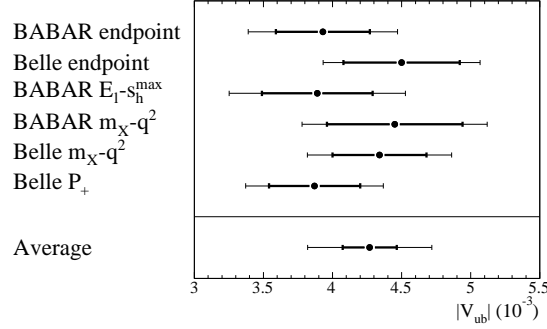


Fig. 2. Results of the inclusive $|V_{ub}|$ measurements. The thick parts of the error bars indicate the experimental errors. The average excludes the Belle P_+ result.

where the errors are experimental, due to the shape function, and theoretical, respectively. The Belle P_+ result is not included in this average because of the strong correlation with the Belle m_X-q^2 result. The overall precision is $\pm 10.5\%$.

The new central value is significantly smaller than the 2004 summer average by the Heavy Flavor Averaging Group, $|V_{ub}| = (4.70 \pm 0.44) \times 10^{-3}$. The change is mainly due to the shape-function parameters, for which the old average used the values extracted from the Belle $b \rightarrow s\gamma$ measurement.¹³ The uncertainty has grown despite the availability of the more precise shape-function parameters. This is partly due to the stronger shape-function dependence of the new theoretical calculation, and also to the more careful assessment of the theoretical uncertainties.¹⁸

The precision of $|V_{ub}|$ from the inclusive measurements is limited by the uncertainties in the shape-function parameters, in particular m_b . The results quoted above assume $\sigma(m_b) = 70\text{--}80\text{ MeV}$, which is probably conservative; as discussed earlier, the latest measurements of $b \rightarrow s\gamma$ can determine m_b to $\pm 40\text{ MeV}$.¹⁴ Using the data samples collected in the next few years, $|V_{ub}|$ may be determined with a precision of $\sim 7\%$.

3. Exclusive Measurements of $|V_{ub}|$

Exclusive measurements of $|V_{ub}|$ can be performed with $B \rightarrow \pi\ell\nu$, $\rho\ell\nu$, $\omega\ell\nu$, $\eta\ell\nu$, etc. Among the possible channels, the $\pi\ell\nu$ decay offers the cleanest path to $|V_{ub}|$ both experimentally and theoretically.

3.1. Theoretical Background

The differential decay rate of the $B \rightarrow \pi\ell\nu$ decay is given by

$$\frac{d\Gamma(B \rightarrow \pi\ell\nu)}{dq^2} = \frac{G_F^2 |V_{ub}|^2}{24\pi^3} |f_+(q^2)|^2 p_\pi^3, \quad (5)$$

where $f_+(q^2)$ is the form factor. We assume from isospin symmetry

$$\Gamma(B \rightarrow \pi \ell \nu) \equiv \Gamma(B^0 \rightarrow \pi^- \ell^+ \nu) = 2\Gamma(B^+ \rightarrow \pi^0 \ell^+ \nu). \quad (6)$$

The form factor $f_+(q^2)$ is significantly harder to calculate than the $B \rightarrow D^*$ and $B \rightarrow D$ form factors. The estimates in literature employ a variety of techniques including quenched lattice QCD (LQCD), light-cone sum rules (LCSR), quark model, and skewed parton distributions. None of the techniques provide robust means of estimating the associated uncertainties.

Two developments in 2004 considerably improved the situation.

- Ball and Zwicky published an improved LCSR calculation.³⁵ They quote a total uncertainty of about 13% in the small- q^2 region ($q^2 < 14 \text{ GeV}^2$).
- Two preliminary results of unquenched LQCD calculations were presented by the HPQCD³⁶ and FNAL³⁷ collaborations. The quoted uncertainties at the large- q^2 region ($q^2 > 15 \text{ GeV}^2$) are about 13% in both cases.

The new calculations should allow reliable determination of $|V_{ub}|$ from $\Gamma(B \rightarrow \pi \ell \nu)$, and stimulated renewed interest in such measurements.

Note that the LQCD and LCSR calculations are valid in limited and non-overlapping regions of q^2 , namely above 15 GeV^2 and below 14 GeV^2 , respectively. Although the authors provide the extrapolation of their calculations to the full q^2 range, such extrapolations add uncertainties that are not fully quantifiable. It is therefore important for the experiments to measure the differential decay rate as a function of q^2 .

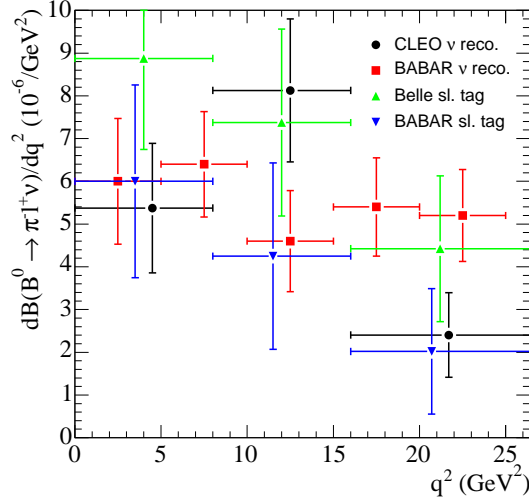
3.2. *Experimental Measurements*

Four measurements of the differential decay rate $d\Gamma(B \rightarrow \pi \ell \nu)/dq^2$ have been reported by CLEO,³⁸ Belle,³⁹ and recently by BABAR⁴⁰ using two different techniques:

- The neutrino reconstruction measurements reconstruct the neutrino as the missing four-momentum of the whole event.
- The semileptonic recoil measurements use the recoil of the B mesons tagged by their semileptonic decays.

Another preliminary measurement by BABAR²⁵ uses the same hadronic recoil technique used in the inclusive $|V_{ub}|$ measurement, and finds $\mathcal{B}(B^0 \rightarrow \pi^- \ell^+ \nu) = (1.08 \pm 0.28 \pm 0.16) \times 10^{-4}$. The statistics of this measurement is too small to allow binning in q^2 .

The neutrino-reconstruction technique has been used by CLEO³⁸ and BABAR.⁴⁰ The momentum of the neutrino is inferred from the missing momentum in the event, and is combined with a lepton and a pion to form a $B \rightarrow \pi \ell \nu$ candidate. The signal is observed as a peak in the (m_B, E_B) plane. The CLEO detector, with a better geometrical coverage than the detectors at the B Factories, is particularly

Fig. 3. Measured $d\mathcal{B}(B^0 \rightarrow \pi^- \ell^+ \nu)/dq^2$.Table 2. Measured $\Delta\mathcal{B}(B^0 \rightarrow \pi^- \ell^+ \nu)$ in low and high regions of q^2 . The errors are statistical, experimental systematic, and due to the $B \rightarrow \rho \ell \nu$ form factors.

	q_{cut}^2	$\Delta\mathcal{B}(q^2 < q_{\text{cut}}^2) \times 10^4$	$\Delta\mathcal{B}(q^2 > q_{\text{cut}}^2) \times 10^4$
CLEO ν reco.	16 GeV^2	$1.08 \pm 0.14 \pm 0.09 \pm 0.04$	$0.25 \pm 0.09 \pm 0.05 \pm 0.03$
BABAR ν reco.	15 GeV^2	$0.85 \pm 0.08 \pm 0.11 \pm 0.05$	$0.53 \pm 0.05 \pm 0.06 \pm 0.03$
Belle sl. tag	16 GeV^2	$1.30 \pm 0.22 \pm 0.15 \pm 0.02$	$0.46 \pm 0.17 \pm 0.05 \pm 0.01$
BABAR sl. tag	16 GeV^2	$0.82 \pm 0.23 \pm 0.12 \pm 0.00$	$0.21 \pm 0.14 \pm 0.06 \pm 0.01$

suited for this technique. The main sources of background are misreconstructed $B \rightarrow X_c \ell \nu$ events and cross-feed from the $B \rightarrow \rho \ell \nu$ decay. The latter makes this type of measurements susceptible to uncertainties of the $B \rightarrow \rho$ form factors.

The semileptonic-recoil technique has been used by Belle³⁹ and BABAR.⁴⁰ The technique is similar to the hadronic-recoil technique, but reconstructs the tag-side B meson in the $B \rightarrow D \ell \nu$ or $D^* \ell \nu$ decays. The efficiency is higher than the hadronic reconstruction by three to four times, thanks to the larger branching fractions of the accessible decay channels. On the other hand, the presence of the extra neutrino makes the kinematics less strongly constrained, resulting in higher background. Overall, this technique provides an efficiency and a signal-to-background ratio that are well matched with the low branching fractions and moderate background levels of the exclusive measurements.

The results of the four measurements agree reasonably well, as shown in Fig. 3. Table 2 summarizes the partial branching fractions in the low- and high- q^2 regions where the LCSR and LQCD calculations are valid, respectively. Note that

Table 3. Values of $\tilde{\Gamma}_{\text{thy}}$ from recent calculations of the $B \rightarrow \pi\ell\nu$ form factor.

	q^2 (GeV ²)	$\tilde{\Gamma}_{\text{thy}}$ (ps ⁻¹)	q^2 (GeV ²)	$\tilde{\Gamma}_{\text{thy}}$ (ps ⁻¹)
Ball-Zwicky	< 15	5.11 ± 1.34	< 16	5.44 ± 1.43
HPQCD	> 15	1.48 ± 0.37	> 16	1.29 ± 0.32
FNAL	> 15	2.01 ± 0.55	> 16	1.83 ± 0.50

Table 4. Values of $|V_{ub}|$ in 10^{-3} from the measurements of $\Delta\mathcal{B}(B^0 \rightarrow \pi^-\ell^+\nu)$ and the recent calculations of the form factor. The errors are due to the $\Delta\mathcal{B}$ measurements and to the form factor calculations.

	Ball-Zwicky	HPQCD	FNAL
CLEO ν reco.	$3.60 \pm 0.28 \pm 0.47$	$3.55 \pm 0.76 \pm 0.44$	$2.98 \pm 0.64 \pm 0.41$
BABAR ν reco.	$3.29 \pm 0.28 \pm 0.43$	$4.83 \pm 0.38 \pm 0.60$	$4.14 \pm 0.33 \pm 0.57$
Belle sl. tag	$3.94 \pm 0.41 \pm 0.52$	$4.82 \pm 0.93 \pm 0.60$	$4.05 \pm 0.78 \pm 0.55$
BABAR sl. tag	$3.13 \pm 0.50 \pm 0.41$	$3.26 \pm 1.18 \pm 0.40$	$2.73 \pm 0.99 \pm 0.37$
Average	$3.49 \pm 0.17 \pm 0.46$	$4.51 \pm 0.31 \pm 0.56$	$3.84 \pm 0.26 \pm 0.53$

the threshold separating the two q^2 regions is different for the *BABAR* neutrino-reconstruction measurement, which uses five q^2 bins instead of three.

3.3. Extraction of $|V_{ub}|$

The measured branching fractions $\Delta\mathcal{B}(B^0 \rightarrow \pi^-\ell^+\nu)$ can be converted into $|V_{ub}|$ using Equation (3) with τ_B replaced by the B^0 lifetime. The reduced decay rate $\tilde{\Gamma}_{\text{thy}}$ is given by

$$\tilde{\Gamma}_{\text{thy}} = \frac{G_F^2}{24\pi^3} \int_{q_{\text{min}}^2}^{q_{\text{max}}^2} |f_+(q^2)|^2 p_\pi^3 dq^2. \quad (7)$$

The values of $\tilde{\Gamma}_{\text{thy}}$ calculated from Ball-Zwicky,³⁵ HPQCD,³⁶ and FNAL³⁷ are given in Table 3. The errors in $\tilde{\Gamma}_{\text{thy}}$ reflects the form-factor uncertainties quoted by the authors. Applying the $\tilde{\Gamma}_{\text{thy}}$ values to the measurements in Table 2, we find the $|V_{ub}|$ values in Table 4 and Fig. 4. The first errors come from the partial branching fraction measurements, and the second from the form-factor calculations. The average $|V_{ub}|$ values in Table 4 were calculated assuming no correlations between the experimental errors. Even for the two *BABAR* measurements, the overlap between the signal samples is small.

Considering only the experimental errors, the measurements of $B \rightarrow \pi\ell\nu$ partial branching fractions can determine $|V_{ub}|$ with a precision better than $\pm 7\%$. The agreement among the existing measurements is satisfactory. The differences among the available form-factor calculations remain considerable, although they are consistent with the quoted theoretical uncertainties.

Historically, the values of $|V_{ub}|$ extracted from the exclusive measurements tended to be smaller than the results of the inclusive measurements. This is no

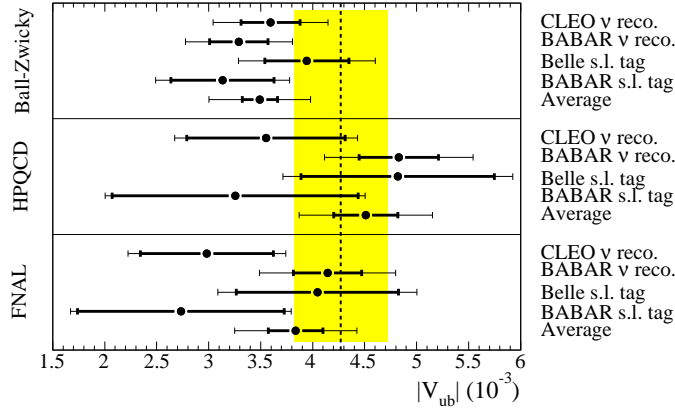


Fig. 4. Values of $|V_{ub}|$ from the measurements of $\Delta\mathcal{B}(B^0 \rightarrow \pi^- \ell^+ \nu)$. The thick part of the error bars correspond to the errors in the $\Delta\mathcal{B}$ measurements. The dashed line and the shaded region indicate the average of the inclusive measurements discussed in Section 2.

longer the case with the latest measurements, partly because the inclusive results have gone down, and partly because the new LQCD results are higher than the older exclusive measurements.

Further improvements in the form-factor calculation are necessary to bring the uncertainty on $|V_{ub}|$ below 10% level. The leading sources of the uncertainties are operator matching and finite lattice spacing for the HPQCD and FNAL calculations, respectively. Technical improvements to overcome these limitations may reduce the total theoretical errors to 5–6% level in the future.⁴¹

3.4. Other Exclusive Measurements

In addition to $B \rightarrow \pi \ell \nu$, the experiments have measured the decay rates for $B \rightarrow \rho \ell \nu$,^{38,39,40,42,43} $B \rightarrow \eta \ell \nu$,³⁸ and $B \rightarrow \omega \ell \nu$.⁴⁴ While the $\rho \ell \nu$ mode has a larger rate than the $\pi \ell \nu$ mode, one must deal with the non-resonant $\pi\pi$ contribution. Theoretically, the $\rho \ell \nu$ mode suffers from the lack of techniques that take into account the width of the ρ resonance. Much progress in LQCD will be necessary before the $B \rightarrow \rho \ell \nu$ decay can be used to extract $|V_{ub}|$ reliably. The $\eta \ell \nu$ and $\omega \ell \nu$ channels, while more challenging to measure, are expected to be more tractable from the theoretical point of view, and may provide valuable cross-checks in the future.

4. Summary and Outlook

A precise determination of $|V_{ub}|$ is one of the most sought-after physics goals pursued at the B factories. The field of charmless semileptonic B decays have seen rapid experimental and theoretical progresses in the last few years. Innovative experimental techniques combined with new theoretical insights have brought the

relative precision of $|V_{ub}|$ close to $\pm 10\%$.

Through the inclusive measurements, we find an average value of $|V_{ub}| = (4.27 \pm 0.45) \times 10^{-3}$. The error is dominated by the uncertainty in the shape function, which can be improved by measurements of the $B \rightarrow X_c \ell \nu$ spectra and of the $b \rightarrow s \gamma$ spectrum. The exclusive $B \rightarrow \pi \ell \nu$ measurements give consistent values of $|V_{ub}|$. The errors are dominated by the $\pm 13\%$ theoretical uncertainties in the form factor.

A 10% precision in $|V_{ub}|$ is almost certainly around the corner. In a few years, with half a billion $B\bar{B}$ events per experiment, it is likely that we will be able to determine $|V_{ub}|$ to a precision of $\sim 7\%$ through the inclusive measurements. Progress in LQCD will eventually achieve a similar precision through the exclusive $B \rightarrow \pi \ell \nu$ measurements, whose experimental precision on $|V_{ub}|$ is already at a 7% level.

Acknowledgments

It is my pleasure to thank P. Fisher, R. Kowalewski and G. Sciolla for their kind help in preparing this article. This work was supported in part by the DOE contract DE-FG02-91ER40654.

References

1. N. Cabibbo, Phys. Rev. Lett. **10**, 531–532 (1963);
M. Kobayashi and T. Maskawa, Prog. Theor. Phys. **49**, 652–657 (1973).
2. J. Charles *et al.* [CKMfitter Group], Eur. Phys. J. C **41**, 1–131 (2005) [arXiv:hep-ph/0406184].
3. I. Bigi and N. Uraltsev, Int. J. Mod. Phys. **A16**, 5201–5248 (2001) [arXiv:hep-ph/0106346].
4. T. van Ritbergen, Phys. Lett. B **454**, 353–358 (1999) [arXiv:hep-ph/9903226].
5. B. Aubert *et al.* [BABAR Collaboration], Phys. Rev. Lett. **93**, 011803 (2004) [arXiv:hep-ex/0404017].
6. P. Gambino and N. Uraltsev, Eur. Phys. J. C **34**, 181 (2004) [arXiv:hep-ph/0401063];
N. Uraltsev, Int. J. Mod. Phys. **A20**, 2099–2118 (2005) [arXiv:hep-ph/0403166].
7. I. Bigi, M. Shifman, N. Uraltsev and A. Vainshtein, Phys. Rev. D **56**, 4017–4030 (1997) [arXiv:hep-ph/9704245].
8. C.W. Bauer, Z. Ligeti, M. Luke, A.V. Manohar and M. Trott, Phys. Rev. D **70**, 094017 (2004) [arXiv:hep-ph/0408002].
9. A.H. Hoang, Z. Ligeti and A.V. Manohar, Phys. Rev. Lett. **82**, 277–280 (1999) [arXiv:hep-ph/9809423];
A.H. Hoang, Z. Ligeti and A.V. Manohar, Phys. Rev. D **59**, 074017 (1999) [arXiv:hep-ph/9811239].
10. M. Neubert, Phys. Rev. D **49**, 4623–4633 (1994) [arXiv:hep-ph/9312311];
I.I. Bigi, M.A. Shifman, N.G. Uraltsev and A.I. Vainshtein, Int. J. Mod. Phys. **A9**, 2467–2504 (1994) [arXiv:hep-ph/9312359].
11. M. Neubert, Phys. Lett. B **612**, 13–20 (2005) [arXiv:hep-ph/0412241].
12. L. Gibbons [CLEO Collaboration], AIP Conf. Proc. **722**, 156 (2004) [arXiv:hep-ex/0402009].
13. A. Limosani and T. Nozaki [Heavy Flavor Averaging Group], arXiv:hep-ex/0407052, 29 July 2004.

14. R. Mommsen [BABAR Collaboration], talk presented at the 40th Rencontres de Moriond on Electroweak Interactions and Unified Theories, 5–12 March 2005.
15. C.W. Bauer, S. Fleming and M.E. Luke, Phys. Rev. D **63**, 014006 (2001) [arXiv:hep-ph/0005275];
C.W. Bauer, S. Fleming, D. Pirjol and I.W. Stewart, Phys. Rev. D **63**, 114020 (2001) [arXiv:hep-ph/0011336];
C.W. Bauer, D. Pirjol and I.W. Stewart, Phys. Rev. D **65**, 054022 (2002) [arXiv:hep-ph/0109045];
M. Beneke, A.P. Chapovsky, M. Diehl and T. Feldmann, Nucl. Phys. B **643**, 431–476 (2002) [arXiv:hep-ph/0206152].
16. F. De Fazio and M. Neubert, JHEP **9906**, 017 (1999) [arXiv:hep-ph/9905351].
17. S.W. Bosch, B.O. Lange, M. Neubert and G. Paz, Nucl. Phys. B **699**, 335–386 (2004) [arXiv:hep-ph/0402094].
18. B.O. Lange, M. Neubert and G. Paz, arXiv:hep-ph/0504071, 11 April 2005.
19. A.K. Leibovich, Z. Ligeti and M.B. Wise Phys. Lett. B **539**, 242–248 (2002) [arXiv:hep-ph/0205148];
C.W. Bauer, M. Luke and T. Mannel, Phys. Lett. B **543**, 261–268 (2002) [arXiv:hep-ph/0205150];
C.W. Bauer, M. Luke and T. Mannel, Phys. Rev. D **68**, 094001 (2003) [arXiv:hep-ph/0102089];
S.W. Bosch, M. Neubert and G. Paz, JHEP **0411**, 073 (2004) [arXiv:hep-ph/0409115];
K.S.M. Lee and I.W. Stewart, Nucl. Phys. B **721**, 325–406 (2005) [arXiv:hep-ph/0409045];
M. Neubert, arXiv:hep-ph/0411027, 1 November 2004;
M. Beneke, F. Campanario, T. Mannel and B.D. Pecjak, JHEP **0506**, 071 (2005) [arXiv:hep-ph/0411395];
F.J. Tackmann, arXiv:hep-ph/0503095, 18 April 2005.
20. I.I. Bigi and N.G. Uraltsev, Nucl. Phys. B **423**, 33–55 (1994) [arXiv:hep-ph/9310285].
21. B. Aubert *et al.* [BABAR Collaboration], arXiv:hep-ex/0408075, 16 August 2004.
22. A. Limosani *et al.* [Belle Collaboration], arXiv:hep-ex/0504046, 26 April 2005.
23. B. Aubert *et al.* [BABAR Collaboration], arXiv:hep-ex/0408045, 12 August 2004.
24. I. Bizjak [Belle Collaboration], talk presented at CKM 2005, Workshop on the Unitarity Triangle, 15–18 March 2005.
25. B. Aubert *et al.* [BABAR Collaboration], arXiv:hep-ex/0408068, 16 August 2004.
26. R. Fulton *et al.* [CLEO Collaboration], Phys. Rev. Lett. **64**, 16–20 (1990).
27. H. Albrecht *et al.* [ARGUS Collaboration], Phys. Lett. B **234**, 409 (1990).
28. A. Bornheim *et al.* [CLEO Collaboration], Phys. Rev. Lett. **88**, 231803 (2002) [arXiv:hep-ex/0202019].
29. K. Abe *et al.* [Belle Collaboration], BELLE-CONF-0325, 2003.
30. R.V. Kowalewski and S. Menke, Phys. Lett. B **541**, 29–34 (2002) [arXiv:hep-ex/0205038].
31. C.W. Bauer, Z. Ligeti, and M.E. Luke, Phys. Rev. D **64**, 113004 (2001) [arXiv:hep-ph/0107074].
32. T. Mannel and S. Recksiegel, Phys. Rev. D **60**, 114040 (1999) [arXiv:hep-ph/9904475].
33. S.W. Bosch, B.O. Lange, M. Neubert and G. Paz, Phys. Rev. Lett. **93**, 221801 (2004) [arXiv:hep-ph/0403223].
34. C. Bozzi [BABAR Collaboration], talk presented at CKM 2005, Workshop on the Unitarity Triangle, 15–18 March 2005.
35. P. Ball and R. Zwicky, Phys. Rev. D **71**, 014015 (2005) [arXiv:hep-ph/0406232].
36. J. Shigemitsu *et al.*, arXiv:hep-lat/0408019, 11 August 2004.

37. M. Okamoto *et al.*, Nucl. Phys. Proc. Suppl. **140**, 461–463, (2005) [arXiv:hep-lat/0409116].
38. S.B. Athar *et al.* [CLEO Collaboration], Phys. Rev. D **68**, 072003 (2003) [arXiv:hep-ex/0304019].
39. K. Abe *et al.* [Belle Collaboration], arXiv:hep-ex/0408145, 30 August 2004.
40. J. Walsh [BABAR Collaboration], talk presented at the 40th Rencontres de Moriond on QCD and High Energy Hadronic Interactions, 12–19 March 2005.
41. J. Shigemitsu, talk presented at CKM 2005, Workshop on the Unitarity Triangle, 15–18 March 2005.
42. B.H. Behrens *et al.* [CLEO Collaboration], Phys. Rev. D **61**, 052001 (2000) [arXiv:hep-ex/9905056].
43. B. Aubert *et al.* [BABAR Collaboration], Phys. Rev. Lett. **90**, 181801 (2003) [arXiv:hep-ex/0301001].
44. C. Schwanda *et al.* [Belle Collaboration], Phys. Rev. Lett. **93**, 131803 (2004) [arXiv:hep-ex/0402023].